Scientific Research Publishing

World Journal of Neuroscience, 2025, 15(4), 356-378
https://www.scirp.org/journal/wjns
ISSN Online: 2162-2019
ISSN Print: 2162-2000

# Analysis and Interpretation of EEG Signals for the Design of an Automated Diagnosis of Disorders of Consciousness and Vigilance through Artificial Neural Network

**Romain Atangana[1,2,3], Ngassa Pelap[3], Amstrong Emini Me Zenanga[3], Daniel Gams Massi[4], Daniel Tchiotsop[1], Godpromesse Kenne[1]**

[1]Unité de Recherche d'Automatique et d'Informatique Appliquée (UR-AIA), IUT of Bandjoun, University of Dschang, Dschang, Cameroun
[2]Unité de Recherche de Matière Condensée d'Electronique et de Traitement du Signal (UR-MACETS), Faculty of Science, University of Dschang, Dschang, Cameroun
[3]Department of Computer Science, Higher Teacher Training College, University of Bertoua, Bertoua, Cameroun
[4]Department of Neurology, Faculty of Health Science, University of Buea, Buea, Cameroon
Email: azongmeromain@gmail.com

**How to cite this paper:** Atangana, R., Pelap, N., Zenanga, A.E.M., Massi, D.G., Tchiotsop, D. and Kenne, G. (2025) Analysis and Interpretation of EEG Signals for the Design of an Automated Diagnosis of Disorders of Consciousness and Vigilance through Artificial Neural Network. *World Journal of Neuroscience*, **15**, 356-378.
https://doi.org/10.4236/wjns.2025.154028

**Received:** May 21, 2025
**Accepted:** November 25, 2025
**Published:** November 28, 2025



## Abstract

Consciousness and vigilance disorders such as coma, vegetative state, and minimally conscious state represent severe neurological conditions that can affect individuals of all ages and sexes. The lack of early diagnosis of these disorders often leads to serious consequences, including impaired driving performance and complications in organ transplantation. This study introduces a new technique for diagnosing consciousness and vigilance disorders based on features extracted from EEG signals using orthogonal polynomial transforms, combined with machine learning paradigms such as artificial neural networks. Current diagnostic approaches suffer not only from limited accuracy but also from challenges in decision-making and delays in obtaining results. Furthermore, they typically require patients to visit medical facilities, where the diagnosis depends on the availability and expertise of specialists. In this work, we propose an automated diagnosis method that allows an individual, based on their EEG parameters, to determine whether they are affected or not. The algorithm also computes relevant metrics such as sensitivity, specificity, and accuracy. The classification task in this study is binary, aiming to distinguish between healthy individuals and patients with disorders of consciousness (DOC), including coma, unresponsive wakefulness syndrome (UWS), and minimally conscious state (MCS). We employ discrete Legendre transforms

to extract discriminative features, which are then classified into two categories: healthy or affected. The results are encouraging, achieving a classification accuracy of up to 75.44% in certain cases using a 10-fold cross-validation technique. Legendre polynomials thus provide a promising tool to complement and improve the detection of consciousness and vigilance disorders. These findings may contribute to enhancing existing state-of-the-art methods for detecting such conditions.

## Keywords

Artificial Neural Network, Coma, Discrete Legendre Transform (DLT), Disorders of Consciousness and Vigilance, EEG Signal, Minimal State of Consciousness, Vegetative State

## 1. Introduction

A disorder of consciousness is an altered state of consciousness, generally caused by injury or dysfunction of the neural systems regulating arousal and awareness [1] [2]. Clinicians and neuroscientists are increasingly seeking to obtain information about brain function from neuroimaging or electrophysiological measurements, in order to achieve a more precise assessment of patients with disorders of consciousness.

Compared with neuroimaging techniques, electroencephalogram (EEG) recordings are more widely applicable. Numerous EEG studies on patients with disorders of consciousness have already been conducted, providing valuable information to clinicians for improving diagnosis, monitoring, and prognosis. However, EEG paradigms, analysis algorithms, and feature extraction methods remain complex.

The analysis of spontaneous EEG activity is an important technique for exploring and evaluating patients with disorders of consciousness, in both acute and chronic conditions. Studies and existing literature highlight the importance of this approach in assessing the severity of brain damage and predicting potential patient outcomes [2] [3]. In addition to conventional visual inspection of EEG traces, several analytical algorithms have been applied to resting EEG signals over the past decades.

The relevance of EEG recording in the evaluation of disorders of consciousness has been recognized since the milestone work of Plum and Posner [4]. The EEG is the most common basic instrumental examination for the diagnosis of brain death continues to be the only procedure that enables bedside monitoring of both "immediate" and long-lasting cortical functioning related to the conscious/unconscious state. Compared with all other neuroimaging techniques, EEG recordings are more widely applicable, less expensive, and provide direct and immediate information.

Consciousness is generally characterized by two main aspects: arousal and con-

scious perception. Arousal is typically defined by spontaneous eye opening or by responses to stimulation (auditory, tactile, or nociceptive) [4]. Importantly, arousal can occur in the absence of consciousness, as some patients may open their eyes without necessarily being aware of themselves or their environment.

The second component, conscious perception (CP), refers to any subjective experience that a person may have. It encompasses both the ability to interact with the environment and self-awareness. CP is associated with functions centralized in the cerebral cortex, particularly those related to affective and cognitive processes [5]. In general, an individual must be awake to exhibit conscious perception. Even individuals without any disorders of consciousness experience fluctuations in wakefulness and conscious perception throughout the day. Under normal conditions, wakefulness and conscious perception are positively correlated, as illustrated in **Figure 1**. When a person is awake, they are generally aware of themselves and their environment.

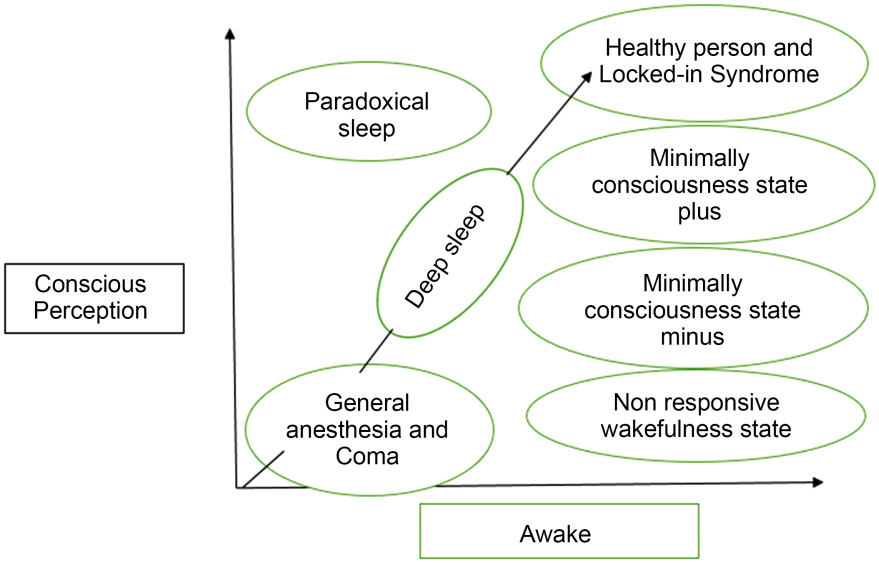


**Figure 1.** The two main components of consciousness: wakefulness and CP.

## 1.1. Altered States of Consciousness

States of altered consciousness correspond to conditions in which the aspects of arousal and conscious perception are either absent or present at varying levels. Typically, a person may enter a coma following a traumatic brain injury. Some of these patients never regain consciousness and die relatively quickly due to the severity of their lesions. However, thanks to technological advances such as the introduction of mechanical ventilation in the 1950s and the development of intensive care units in the 1960s the majority of patients now open their eyes and emerge from coma.

The main states of altered consciousness are coma, unresponsive wakefulness syndrome, and the minimally conscious state. These conditions are characterized by precise diagnostic criteria established by groups of specialized researchers.

### 1.2. Coma

Coma is characterized by a complete absence of both wakefulness and awareness of oneself and the environment [4]. To distinguish coma from syncope, concussion, or transient loss of consciousness, the condition must persist for at least one hour and may last for several weeks. According to Howard [5], coma is characterized by closed eyes, no spontaneous eye opening, and no reaction to external stimulation. Patients who do not die may progress within two to four weeks to different states, such as unresponsive wakefulness syndrome, minimally conscious state, or locked-in syndrome.

### 1.3. Brain Death State

From a neurological perspective, this state corresponds to brain death. It is characterized by a preceding coma, the absence of brainstem reflexes and motor responses, and the presence of apnea, in the absence of confounding factors such as hypothermia, drugs, or endocrine and electrolyte disorders. One of the main tools recommended to confirm the diagnosis is electroencephalography [6] [7], which should demonstrate cortical silence, thereby confirming the absence of neuronal activity throughout the brain.

### 1.4. Unresponsive Wakefulness State

The unresponsive wakefulness state (UWS), previously referred to as the vegetative state (VS), is characterized by the presence of wakefulness but the absence of conscious perception and cognition. UWS includes intermittent spontaneous opening and closing of the eyes, along with the absence of reproducible voluntary behavior. The term *vegetative state* was introduced more than 45 years ago by Jennett and Plum, referring to the preservation of vegetative nervous system functions [8]. It is difficult to identify specific lesional areas for UWS, as these are strongly influenced by the underlying etiology [9].

### 1.5. Minimally Conscious State

The term minimally conscious state (MCS) was introduced approximately fifteen years ago to describe patients who are awake and exhibit more complex signs of consciousness. This state is characterized by marked fluctuations in signs of consciousness, which can vary from moment to moment. Depending on the complexity of these signs of consciousness in MCS patients are further divided into two categories, each with precise diagnostic criteria: MCS minus (MCS−) and MCS plus (MCS+). Patients in MCS− exhibit low-level signs of consciousness corresponding to non-reflex, goal-directed behaviors, whereas patients in MCS+ show higher-level responses, including movements in response to yes/no commands, gestural or verbal responses, or intelligible verbalization.

Similar to the unresponsive wakefulness state, the minimally conscious state can be either transient or chronic. Some patients may remain in this state for several years and gradually regain normal consciousness. Diagnosis can only be con-

firmed when one of the two criteria communication or functional use of objects is observed on two consecutive behavioral evaluations.

### 1.6. Locked-in Syndrome (LIS)

The term locked-in syndrome (LIS) was introduced in the 1980s by Plum and Posner to describe a neurological condition in patients who are completely paralyzed but awake, exhibiting a level of consciousness comparable to that of individuals without neurological deficits [10]. Since then, the definition has been refined, and three distinct diagnostic categories are currently recognized: classic LIS, incomplete LIS, and total LIS, which are distinguished by the absence (total LIS) or presence (classic and incomplete LIS) of minimal motor functions.

The main criteria for diagnosing classic LIS include the preservation of eye opening, the ability to communicate via eye movements and/or blinking, quadriplegia or hypophonia, and relatively preserved cognitive functions.

## 2. Related Works

Neuroimaging techniques such as PET and MRI are valuable for detecting the brain networks underlying residual consciousness abilities. However, electroencephalography offers additional advantages that are particularly useful for studying altered states of consciousness and the associated neuronal activities.

EEG studies have notably demonstrated that electrogenesis in patients with altered consciousness is accompanied by an increase in slow delta-type waves [11] [12]. Lehembe *et al.* demonstrated higher delta spectral power in unresponsive wakefulness state (UWS) patients compared to those in the minimally conscious state (MCS). These authors also observed reduced brain connectivity between different electrodes.

More recently, Bagnato *et al.* [13] reported that a reduction in EEG amplitudes and delta frequencies is associated with an absence of UWS or fewer behavioral signs three months post-etiology, whereas alpha frequencies and reactivity correlate with a greater number of behavioral signs of consciousness.

EEG studies conducted on LIS patients have shown more heterogeneous results. Gutling *et al.* [14] studied and published the clinical and neurophysiological data of five LIS patients. They found that EEG reactivity was present in two of these patients but absent in the remaining three.

A multicenter study by Estraneo *et al.* [15] predicted patient outcomes using EEG reactivity to eye opening and closing as well as acoustic stimuli, defined as a reproducible change in signal frequency or amplitude within a 3-second epoch. The predictive power of these measures was superior to that obtained using tactile and noxious stimuli or evoked potentials, including event-related potentials (ERP).

Chen *et al.* [16] reported the significant prognostic value of post-stimulation EEG reactivity across different frequency bands and changes in connectivity. These measures were strongly correlated with patient outcomes when evaluated

after "quantifiable" electrical stimulation using 5 Hz square-wave pulses lasting 2 seconds above the motor threshold.

In the current clinical context, EEG reactivity with relatively simple stimulus protocols provides an easy and noninvasive method for assessing peripheral and central ascending sensory pathways, offering partial but useful information about the functional integrity of the brainstem, thalamus, and cerebral cortex [17].

Several studies have investigated resting EEG using non-linear analyses based on indices such as complexity and entropy [18]. Entropy, which measures signal regularity, provides intuitive metrics that are potentially suitable for clinical interpretation. High entropy values indicate that a subject exhibits a less regular (more variable) EEG at rest, suggesting a state closer to wakefulness, whereas lower values are associated with unconscious states [19].

Various algorithms have been applied to calculate entropy, including Lempel–Ziv complexity, approximate entropy, and cross-entropy, yielding consistent and promising results both for distinguishing between UWS/VS and MCS patients [20] and for correlating with different r-CRS scores [21] [22].

Andrea Piarulli *et al.* (2016) [23] analyzed 4-hour EEG recordings from 12 patients with disorders of consciousness (6 MCS and 6 vegetative state/unresponsive wakefulness syndrome - VS/UWS). Relative powers (delta, theta, alpha, beta1, beta2 bands) and spectral entropy were estimated. Spectral entropy time courses were then analyzed. MCS patients had higher theta and alpha and lower delta power when compared to VS/UWS. They also showed higher mean spectral entropy values and greater time variability. MCS patients were characterized by spectral entropy fluctuations with periodicity of approximately 70 minutes (range 57 - 80 minutes).

Monti MM, Laureys S, and Owen AM (2010) [18] aimed to classify the EEG literature on patients with disorders of consciousness according to protocols, analysis methods, and clinical utility. Klimesch W. (1999) [3] and Busch NA, Van Rullen R. (2010) [24] highlighted the significance of EEG spectral power. Spontaneous EEG oscillations can be divided into several frequency bands, generally as follows: delta (0.5 - 4 Hz), theta (4 - 8 Hz), alpha (8 - 13 Hz), beta (13 - 30 Hz), and gamma (>30 Hz). Given their specific roles in different brain functions, the power of these frequency bands is typically highly abnormal in patients with disorders of consciousness.

Rossi Sebatiano D; Panzica F; Visani E, Rolant F; Scaica V; Leonardi M *et al.* (2015) [25] explain how enhanced delta and suppressed alpha activities have been highlighted as markers of low consciousness level. The delta power in disorder of consciousness patients is higher than in healthy controls.

Several studies have investigated EEG spectral power in patients with disorders of consciousness. Lechinger *et al.* (2013) [26] and Sitt *et al.* (2014) [27] reported that spectral power is dominated by the delta band in nearly 80% of VS/UWS patients. Naro *et al.* (2018) [28] found that theta power is increased in VS/UWS patients compared to healthy controls, and also elevated in MCS patients compared

with healthy or fully conscious individuals. Similarly, Leon-Carrion *et al.* (2008) [20] observed higher theta power in MCS patients compared to VS/UWS patients.

The depression of alpha power is more pronounced in VS/UWS patients than in MCS patients. Naro *et al.* (2016) reported that alpha power in MCS patients is significantly higher than in VS/UWS patients. Schorr *et al.* (2018) [26] and Lehembre *et al.* (2012) showed that alpha power can be up to twice as high in the central, parietal, and occipital regions of MCS patients compared to VS/UWS patients. Ressi *et al.* demonstrated that residual consciousness in patients with disorders of consciousness correlates strongly with alpha power in frontal and parietal networks. Chennu *et al.* (2012, 2016) [29] further reported that an increase in alpha power over time is associated with a higher likelihood of conscious recovery.

## 3. Materials and Methods

### 3.1. Software and Hardware Equipment

For the simulations in this study, we used an HP laptop with the following specifications: Intel Core i5 processor with 5 cores running at 2.3 GHz, 500 GB SSD, 4 GB RAM, and Windows 10 64-bit operating system. The simulations were conducted using MATLAB R2022a, which includes several toolboxes for machine learning, allowing us to perform automatic classification tasks efficiently.

### 3.2. Dataset Description

The data used in this study are part of Coralie Joucla's dataset [30], which demonstrates that several characteristics of brain activity can be extracted. The initial dataset included 1217 participants, comprising 681 patients with disorders of consciousness (DOC) and 588 healthy control subjects (Non-DOC). Continuous EEG recordings were obtained for each participant. To make these signals suitable for automated analysis, the recordings were preprocessed to correct or remove artifacts, including ocular movements, muscle contractions, and electrode-related noise.

After preprocessing, the EEG signals were segmented into 5-second temporal windows. To increase the number of learning instances while preserving temporal continuity, a 50% overlap was applied between consecutive windows. Each window was treated as an individual unit of analysis for the deep learning stage.

**Table 1.** Events studied with the EEG signals.

| Events | Definition | Comments |
|---|---|---|
| Coma | Vigilance disorder | Patient with eyes closed, he is unaware of himself. |
| Vegetative state | Consciousness disorder | Patient with eyes open, unaware of himself, awake state and sleep preserved. |
| Minimally conscious state | Consciousness disorder | Patient with eyes open, he is unaware of himself but reacts to stimuli. |

Following segmentation with overlap, approximately 4000 EEG samples were obtained, balanced between DOC patients and Non-DOC subjects. These samples constituted the dataset used for training, validation, and testing of our artificial neural network model (Table 1).

## 3.3. Mathematic Fundamental Principles

### 3.3.1. Generalities on Orthogonal Polynomials

Orthogonal polynomials play an important role in spectral analysis, so it is important to understand their general properties. Orthogonal polynomials constitute families of spaces $L_w^2[a,b]$ with $\mathrm{d}\omega = \omega \mathrm{d}x$.

Consider an interval $[a,b]$, and a weight function $\omega(x) > 0$ in $[a,b]$, and $\omega \in L_1[a,b]$. For any arbitrary function $f(x) \in [a,b]$ to be expanded in terms of Fourier series following an orthogonal polynomials family $\{P_k(x)\}$ on $[a,b]$, it is necessary that $f(x) \in [a,b]$, and that:

$$\int_a^b f^2(x)\omega(x)\mathrm{d}x < +\infty \tag{1}$$

If $f(x)$ satisfies the previous condition, it is an integrable square function and, in theory of signal, $f(x)$ corresponds to a finite energy signal. Several other notions on the development in Fourier series in Hilbert spaces can be found in Tchiotsop [31].

There fore, it becomes obvious that the scalar function $(.,.)_\omega$, defined by:

$$(f,g)_\omega = \int_a^b f^2(x)g(x)\omega(x)\mathrm{d}x < +\infty \tag{2}$$

The inner product in $L_w^2[a,b]$ is defined as:

$$\|f\|_{L_w^2} = (f,f)_\omega^{\frac{1}{2}} \tag{3}$$

Two functions *f* and *g* are orthogonal in $L_w^2[a,b]$ if:

$$(f,g)_\omega = 0 \tag{4}$$

A sequence of polynomials $\{P_n\}_{n=0}^L$ is said to be orthogonal in $L_w^2[a,b]$:

$$(p_i, p_j)_\omega = C_i^2 \delta_{ij}$$

where $C_i = \|P\|_{L_w^2}$ and $\delta_{ij}$ is the Kronecker delta: $\delta_{ij} = \begin{cases} 1, & \text{if } i = j \\ 0, & \text{otherwise} \end{cases}$

For the discrete case, let the weight function $\omega(x) > 0$, and $\{x_j, \omega_j\}_{j=0}^{N-1}$ be a sequence of *N* points. The discrete scalar product and norm are defined as:

$$\langle u,v\rangle_{N,\omega} = \sum_{j=0}^{N-1} u(x_j)v(x_j)\omega_j \tag{5}$$

$$\|U\|_{N,\omega} = (N,N)_{N,\omega}^{\frac{1}{2}} \tag{6}$$

Here, $\langle .;. \rangle_{N,\omega}$ and $\|.\|_{N,\omega}$ represent the discrete inner product and norm in $P_N$.

### 3.3.2. Generalities on Legendre Polynomials

There are several families of orthogonal polynomials, including the Laguerre, Hermite, and Jacobi polynomials. Jacobi polynomials are a very large class of orthogonal polynomials with interesting properties for biomedicine, making them attractive for optimal polynomial interpolation.

These polynomials are orthogonal on the interval [−1, 1] with the weight function (for $\alpha, \beta > 1$):

$$\omega(x) = (1+x)^{\alpha}(1+x)^{\beta} \tag{7}$$

The Jacobi family is divided into two main subfamilies: Chebyshev polynomials and Legendre polynomials.

In this work, we focus on first-order Legendre polynomials, denoted by $L_n$. The differential equation for Legendre polynomials is given by:

$$\frac{\mathrm{d}}{\mathrm{d}x}\left[\left(1-x^2\right)\frac{\mathrm{d}}{\mathrm{d}x}L_n(x)\right] + n(n+1)L_n(x) = 0, n \in N. \tag{8}$$

The recurrence formula is:

$$\begin{cases} L_0 = 0 \\ L_1 = x \\ L_{n+1}(x) = \dfrac{2n+1}{n+1}x * L_n(x) - \dfrac{n}{n+1} * L_{n-1}(x) \end{cases} \tag{9}$$

The polynomial $L_n(x)$ can also be defined by Rodrigues' formula:

$$L_n(x) = \frac{1}{2^n n!}\frac{\mathrm{d}^n}{\mathrm{d}x^n}\left[\left(1-x^2\right)^n\right]$$

### 3.3.3. Expansion of the Signal into the Legendre Orthogonal Base

The polynomial projection of a signal $s(x)$ onto the Legendre orthogonal basis of order $M$ is given by:

$$s(x) = \sum_{k=0}^{M} \alpha_k L_k(x) \tag{10}$$

where the sequence of coefficients $\{\alpha_k\}_{k=0}^{M}$ are the spectral coefficients of the signal decomposition or projection into the Legendre polynomial basis and are evaluated by:

$$\begin{aligned} \alpha_k &= \frac{\langle s(x), L_k(x)\rangle}{\langle L_k(x), L_k(x)\rangle} = \frac{\langle s, L_k(x)\rangle}{\langle L_k(x), L_k(x)\rangle} \\ &= \frac{\int_{-1}^{1} s(x)L_k(x)\mathrm{d}x}{\int_{-1}^{1} L_k^2(x)\mathrm{d}x} = \frac{1}{d_k^2}\int_{-1}^{1} s(x)L_k(x)\mathrm{d}x \end{aligned} \tag{11}$$

With:

$$d_k^2 = \frac{2}{2k+1}$$

The evaluation of the coefficients $\alpha_k$ is done efficiently with the Gauss-Lo-

batto method, which is a powerful tool for numerical integration, especially dedicated to orthogonal polynomials. Thus, Gaussian quadrature states that for a family of orthogonal polynomials $\{P_k(x)\}$ in the interval $[a,b]$, with respect to the weight function $\omega(x)$ the following approximation is made:

$$\int_a^b f(x)\omega(x)\mathrm{d}x = \sum_{j=0}^{M} G_j f(x_j) \tag{12}$$

where $f(x) \in L^2[a,b]$ are the $M+1$ nodes of $P_{M+1}(x)$ and $G_j$ are the coefficients or weights of Gauss, called "Christoffel numbers".

$$\int_{-1}^{1} s(x)L_k(x)\mathrm{d}x = \frac{2}{M(M+1)}\sum_{j=0}^{M}\frac{s(x_j)L_k(x_j)}{\left[L_M(x_j)\right]^2} \tag{13}$$

where $x_j$ are the $M+1$ Gauss-Lobatto nodes of $(1-x^2)L_M(x)$, formed by $x_0=-1$, $x_M=1$, and $x_j$ for ($j=1,2,\cdots,M-1$) calculated by the eigenvalue method. The Christoffel numbers are given by:

$$G_j = \frac{2}{M(M+1)}\frac{1}{\left[L_M(x_j)\right]^2}, \tag{14}$$

After application of the Gauss-Lobatto method, the spectral coefficients of decomposition are given by the following equation, which characterizes the DLT:

$$\begin{cases} \alpha_k = \dfrac{2k+1}{M(M+1)}\displaystyle\sum_{j=0}^{M}\frac{L_k(x_j)}{\left[L_M(x_j)\right]^2}s(x_j), k=0,1,\cdots,M \\ \alpha_M = \dfrac{1}{M+1}\displaystyle\sum_{j=0}^{M}\frac{s(x_j)}{L_M(x_j)}, k=M \end{cases} \tag{15}$$

### 3.4. Methodology Used

The methodology used is described below as shown in the following block diagram (**Figure 2**).

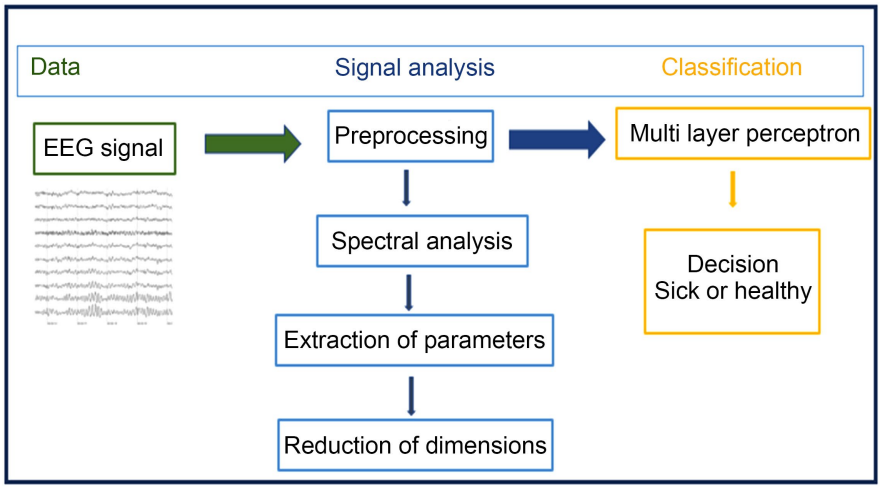


**Figure 2.** Steps of signal processing for the detection.

### 3.4.1. Data Preprocessing

Electrical signals in the EEG that originate from non-cerebral sources are referred to as artifacts. EEG data are almost always contaminated by such artifacts, which typically have amplitudes higher than the signals of interest. This is one reason why considerable experience is required to correctly interpret EEGs in a clinical context.

At this stage, the data were reorganized to generate multiple samples, facilitating subsequent processing and analysis (Figure 3).

| Characteristics | | Sample N = 4000 | |
|---|---|---|---|
| | | Patients with disorders of consciousness (DOC) | Healthy persons (Non-DOC) |
| Gender | Male | 14 | 12 |
| | Femel | 15 | 14 |
| gronbling | Thrut | 16 | 03 |
| | false | 13 | 23 |
| Snesory movment | left | 14 | 00 |
| | rigth | 08 | 00 |
| | none | 07 | 26 |
| Impact | none | 01 | 23 |
| | Beginner | 19 | 03 |
| | averagen | 07 | 00 |
| | sever | 02 | 00 |
| Lévodopa | thrut | 00 | 00 |
| | false | 29 | 26 |
| Total Numbers of patients | | 29 | 26 |

Figure 3. General description of the data.

At the end of the procedure, the reorganized DataSet contains 588 healthy persons and 681 patients with disorders of consciousness within a sample of 4000 persons.

### 3.4.2. Spectral Analysis

To transform the EEG signals from the time domain to the frequency domain, we employed the Discrete Legendre Transform (DLT). Unlike the Fourier transform, which is less suitable for non-stationary signals, the DLT enables localized analysis and effectively handles non-periodic and broadband phenomena. The data were interpolated using the DLT with an approximation order set to twice the data

length plus one, ensuring minimal approximation error and maximal preservation of the original signal information. This choice of DLT was primarily made for comparative purposes, although we have also successfully applied the wavelet transform in previous EEG studies.

### 3.4.3. Feature Extraction

After decomposing the EEG signals using the Legendre orthogonal basis, we extracted statistical features designed to capture relevant information from the recordings. These features provide a distinctive characterization of brain activity during the corresponding tasks, enabling differentiation between healthy individuals and patients with disorders of consciousness.

EEG frequency reflects the repetitive rhythmic activity of the brain (in Hz), which varies across different states such as wakefulness and sleep. Traditionally, frequency information is extracted using the Fast Fourier Transform (FFT), wavelet transforms, Common Spatial Patterns (CSP), or their derivatives. In this study, we employed the Discrete Legendre Transform (DLT) for feature extraction, as it effectively captures transient, nonstationary, and broadband components of the EEG signal. From the DLT coefficients, we computed several statistical parameters, including peak factor, latency factor, and other relevant measures that correlate with the patient's level of consciousness.

- **The peak factor (DP):** It is the ratio between the maximum absolute value and the square root of average power, which for a set $X$ of $N$ elements is defined as:

$$\mathrm{DP} = \frac{\max\left(|x|\right)}{\sqrt{\frac{\sum_{i=1}^{N} X_i^2}{N}}}$$

- **The mean ( $\bar{X}$ ):** It is a calculation tool allowing a list of numerical values to be summarized into a single real number. Its formula is:

$$\bar{X} = \frac{1}{N}\sum_{i=0}^{N} X_i$$

- **The Median (Me):** It is the value which separates the lower half from the upper half in a set. For a set $X$ of $N$ elements:

$$\mathrm{Me}(x) = \begin{cases} X\left[\frac{N}{2}\right], & \text{if } N \text{ is odd} \\ \frac{X\left(\frac{N-1}{2}\right) + X\left(\frac{N+1}{2}\right)}{2}, & \text{if } N \text{ not odd} \end{cases}$$

- **The mode (Mo):** It is the most frequent value in a given set.
- **The 1st quartile (1er qr):** The data value that separates the lowest 25% of the data.
- **The 3rd quartile (3me qr):** The data value that separates the lowest 75% of the data.
- **The interquartile range (IQR):** The difference between the 3rd quartile and

the 1st quartile.

- **The absolute deviation median ($mad_2$):** It is the median of the absolute values of the deviations between each value and the median. For a set $X$ of $N$ numbers, it is defined as:

$$\mathrm{mad}_2 = \mathrm{Met}\left(\left|X_i - \mu\right|\right)$$

where $\mu$ represents the mean of the set $X$.

- **Entropy of Shannon (ShEn):** It corresponds to the quantity of information contained or delivered by an information source. It is defined by:

$$H_b = -\sum_{i=1}^{n} P_i \log_b\left(P_i\right)$$

- **The Latitude Factor (LF):** It is the ratio between the maximum absolute value and the average value, for a set $X$ of $N$ elements:

$$\mathrm{IF} = \frac{N * \max\left(\left|X\right|\right)}{\frac{1}{N}\sum_{i=1}^{N} X_i}$$

- **Percent Root Difference (PRD):** It is a widely used parameter for measuring reconstruction fidelity. It determines the percentage of relative normalized error in energy and quantifies the quality of the reconstructed signal. For a signal $\{S_n\}_{n=1,2,\ldots}$. and the approximated signal $\{Se_n\}_{n=1,2,\ldots}$, it is expressed as:

$$\mathrm{PRD}(\%) = 100\sqrt{\frac{\sum\left(S_n - \widetilde{S_n}\right)^2}{\sum\left(S_n\right)^2}}$$

### 3.4.4. Dimensionality Reduction

To reduce dimensionality and select relevant features, Principal Component Analysis (PCA) was employed. PCA is a linear transformation technique that extracts essential information from the original dataset and provides a roadmap for dimensionality reduction.

The primary goal of PCA is to reduce a d-dimensional dataset by projecting it onto a k-dimensional subspace, where $k \leq d$. PCA is an unsupervised algorithm, as it ignores class labels and identifies the principal components directions of maximum variance in the high-dimensional data there by minimizing information loss when projecting onto a lower-dimensional subspace.

This approach improves computational efficiency, reduces noise and redundancy, and retains most of the relevant information from the original data. The first principal component captures the maximum variance. Consequently, the features selected by PCA are non-redundant and serve as the input for the classifier used in subsequent analyses.

Although multiple disorders of consciousness (DoC) are considered in this study, including coma, UWS, and MCS, the classification task is performed in a binary manner, distinguishing healthy individuals from patients with DoC (**Figure 4**).

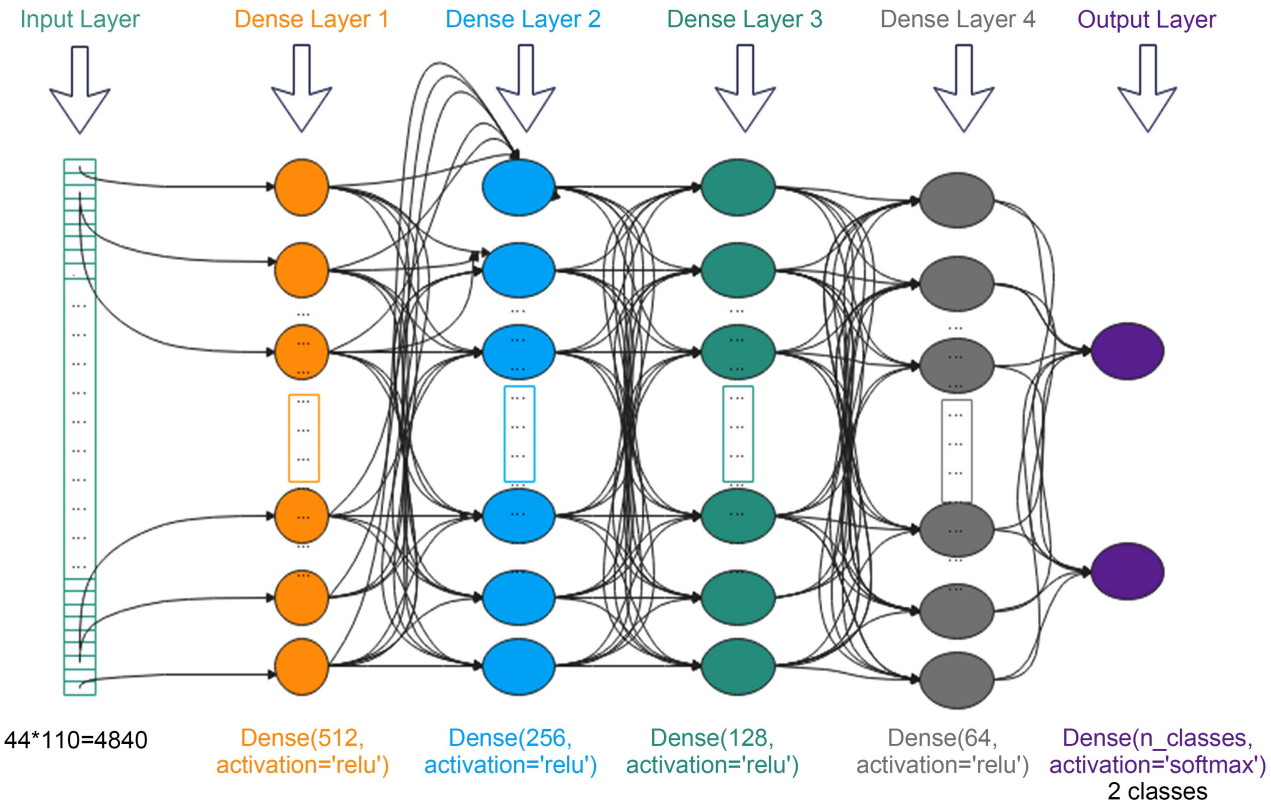


**Figure 4.** Classification architecture.

**1) Architecture**

*a*) *Input*: *Input Layer*

- **Input Dimension:** $n_{\text{channel}} * time_{\text{steps}}$ .
- **Example:** If we have 64 EEG channels and 100 points per time window, the input will have a dimension of 64 × 100 = 640064.

*b*) *Dense Layer* 1

- **Dense Layer:**
- **Description:** First fully connected layer which takes the flattened features as input.
- **Hyperparameters:**
  - Units: 512
  - Activation Function: ReLU (non-linear activation function)
- **Batch Normalization:** Normalizes activations to improve stability and speed of training.
- **DropOut:** is applied to avoid overfitting.

*c*) *Dense Layer* 2

- **Dense Layer:**
- **Description:** Second fully connected layer.
- **Hyperparameters:**
  - Units: 256
  - Activation Function: ReLU

- **DropOut:**

*d*) *Dense Layer* 3

- **Dense Layer:**
- **Description:** Third fully connected layer with reduced size.
- **Hyperparameters:**
  - Units: 128
  - Activation Function: ReLU

*e*) *Output*: *Output Layer*

- **Dense Layer:**
- **Description:** Output layer for classifying states of consciousness.
- **Hyperparameters:**
  - n_Classes: Number of classes.

**2) Hyperparameters**

- **Batch Size:** 32 or 64 (depending on the size of the data).
- **Optimizer:** Adam with an initial learning rate of $10^{-3}$.
- **Loss Function:** Categorical Cross-Entropy for multiclass classification.
- **Epochs:** 50 to 100 (depending on convergence).

## 4. Results

### 4.1. Results of Sample Decomposition

After reorganizing the dataset, we obtained a total of 4000 samples from both healthy individuals and patients with disorders of consciousness. Each sample is labeled according to the corresponding condition: Coma, Vegetative State (VS), or Minimally Conscious State (MCS).

Figure 5 below illustrates the time-domain graphs for each state.

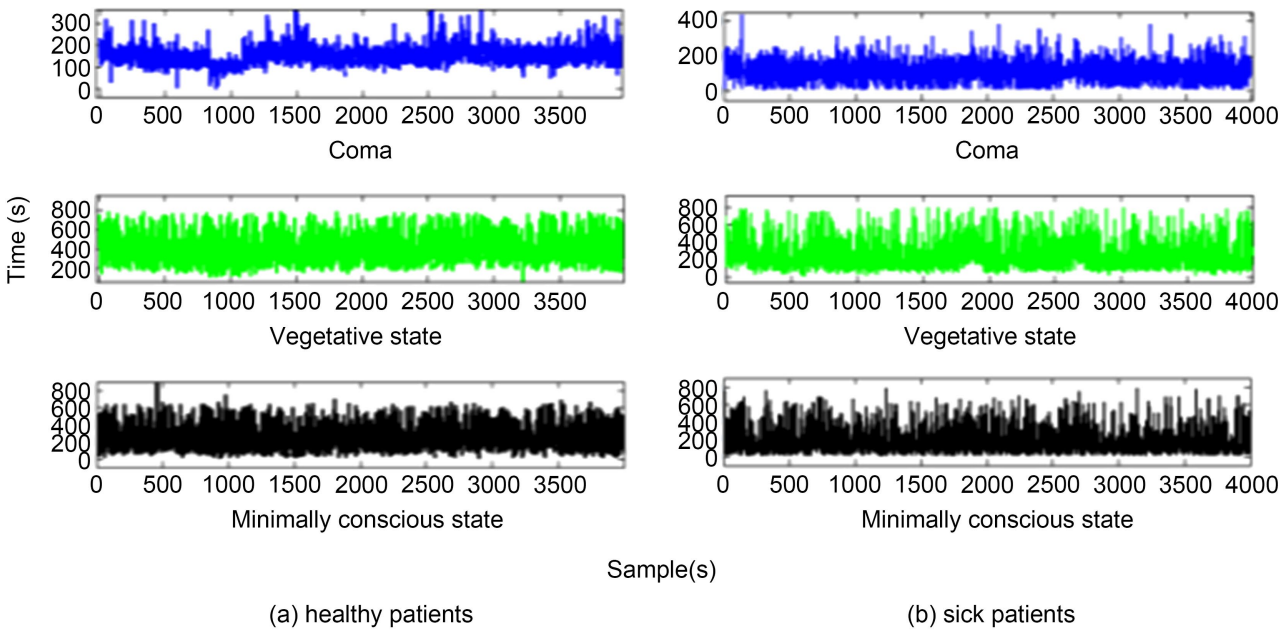


Figure 5. Recordings EEG signals for healthy (a) and patients with disorder of consciousness (b).

### 4.2. Results of Spectral Analysis

After the preprocessing stage, spectral analysis represents the second step of the proposed methodology. The signals were interpolated, and their frequency distributions were expressed in terms of spectral Legendre decomposition coefficients.

Figure 6 below illustrates the differences between the original signals and the reconstructed signals. The Percentage Root-Mean-Square Difference (PRD) in this figure is less than 1%, demonstrating that Legendre polynomials are an effective tool for spectral analysis.

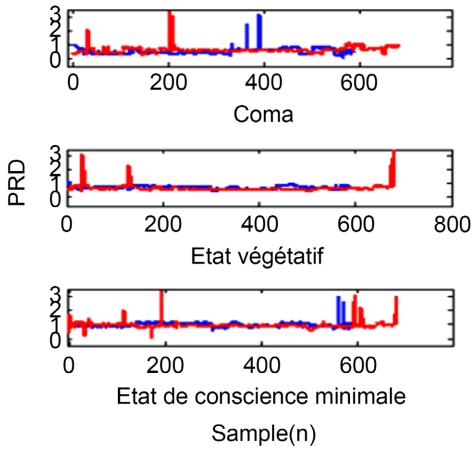


Figure 6. Difference between original signal and reconstructed signal.

### 4.3. Results of Feature Extraction

After spectral analysis, the next step is to extract relevant features from the signal. These features include the mean, median, Shannon entropy, among others.

Figure 7 and Figure 8 present the results obtained in 1D and 2D after feature extraction for both healthy individuals and patients with disorders of consciousness. The blue curves represent *healthy subjects*, while the red curves represent *patients* for each condition: Coma, Vegetative State, and Minimally Conscious State (MCS).

### 4.4. PCA Results

After processing the signals using spectral analysis with the Discrete Legendre Transform, each of the three events in a signal is represented by a feature vector of 85 elements, reducing the dimensionality from 8001 to 85.

In summary:

- Each event in the healthy group is represented as a matrix of size 588 × 85.
- Each event in the group of patients with disorders of consciousness is represented as a matrix of size 681 × 85.

After applying Principal Component Analysis to the vector of statistical parameters extracted from the DLT coefficients, 13 principal components were selected to reduce redundancy and retain the most informative features.

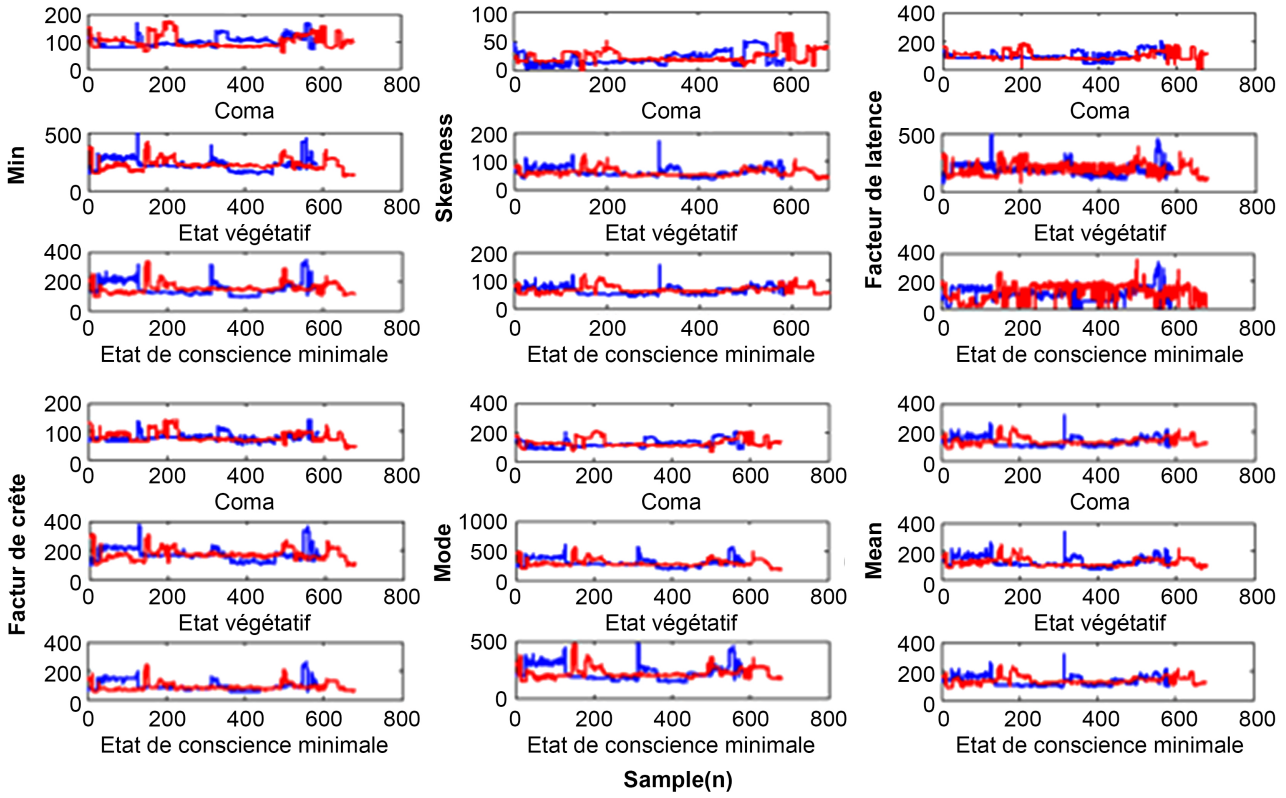


Figure 7. Some parameters 1-D.

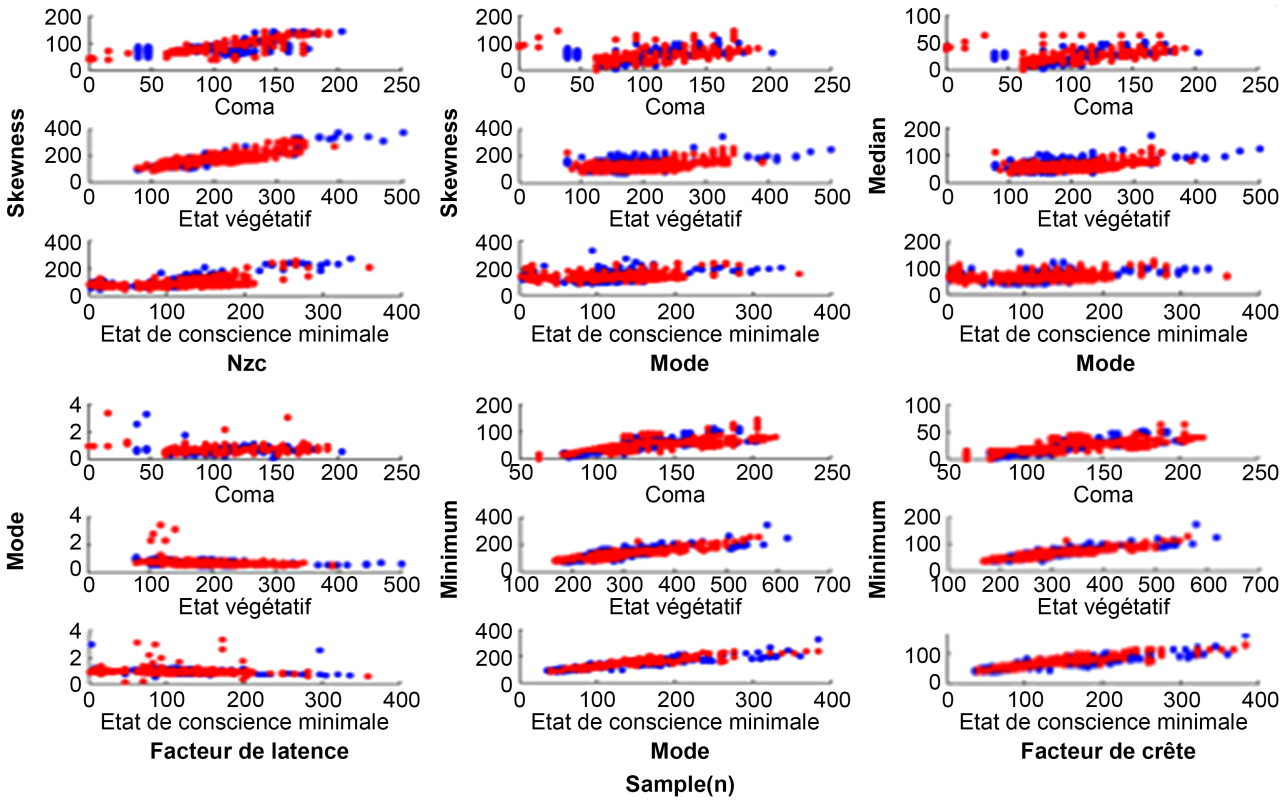


Figure 8. Some parameters 2-D.

These 13 components were then used as input to the classifier. The cumulative variance explained by these components was calculated by summing their corresponding eigenvalues, ensuring that a substantial portion of the original signal variability was preserved.

In this study, we employed a multilayer perceptron neural network with a single hidden layer and a sigmoid activation function. For classification, 60% of the data from each class were used to form the training set, while the remaining 40% constituted the test set. In addition, a 10-fold cross-validation procedure was applied to the training set to determine the optimal parameters of the neural network, such as weights and biases.

During this procedure, each fold was used once as a validation set, while the remaining nine folds served as the training data. The classifier parameters were estimated iteratively across all ten folds. This process was repeated ten times, producing ten distinct sets of classifier parameters, from which the optimal configuration was selected.

The performance metrics of the classifier, including accuracy, precision, recall, and F1-score, are summarized in Table 2 below.

**Table 2.** Evaluation of metrics.

| Dimension | Metrics % | C1 | C2 | C3 | C4 | C5 | C6 | C7 | C8 | C9 | C10 | C11 | C12 |
|---|---|---|---|---|---|---|---|---|---|---|---|---|---|
| 1 | Sen | 85.66 | 99.63 | 84.55 | 100 | 88.97 | 97.05 | 61.78 | 99.54 | 91.91 | 100 | 100 | 100 |
| 1 | Sep | 22.55 | 95.74 | 85.95 | 60.30 | 66.30 | 82.12 | 94.45 | 100 | 26.48 | 99.57 | 100 | 100 |
| 1 | Acc | 55.22 | 60.35 | 65.48 | 63.51 | 66.27 | 62.91 | 61.74 | 54.64 | 57.19 | 54.65 | 74.48 | 74.44 |
| 2 | Sen | 66.88 | 97.54 | 81.91 | 99.56 | 100 | 71.79 | 98.46 | 67.78 | 100 | 100 | 100 | 100 |
| 2 | Sep | 96.98 | 100 | 66.48 | 98.57 | 100 | 100 | 84.58 | 100 | 46.79 | 96.57 | 100 | 100 |
| 2 | Acc | 71.84 | 64.64 | 67.19 | 66.65 | 74.68 | 75.44 | 65.74 | 62.78 | 65.22 | 71.67 | 74.48 | 74.44 |

### 4.5. Classification Results

After feature extraction and selection, the low-dimensional parameter vectors were used as input to a classifier consisting of a multilayer perceptron neural network with a single hidden layer and a sigmoid activation function.

For classification:

- 60% of the data from each class was used to form the training set.
- The remaining 40% constituted the test set.
- A 10-fold cross-validation was applied to the training set to determine the optimal parameters (weights and biases) of the artificial neural network.

After extraction and selection of relevant features, the low-dimensional parameter vectors were directly used as input to the classifier. In this study, we employed a multilayer perceptron architecture for efficient classification of the EEG signals.

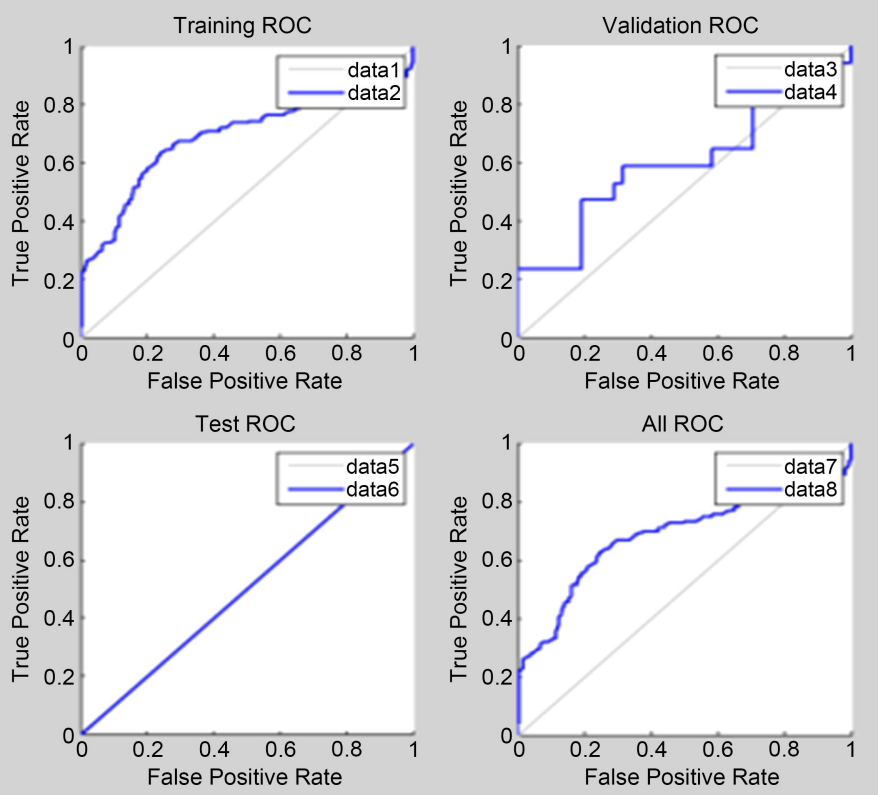


**Figure 9.** ROC curves.

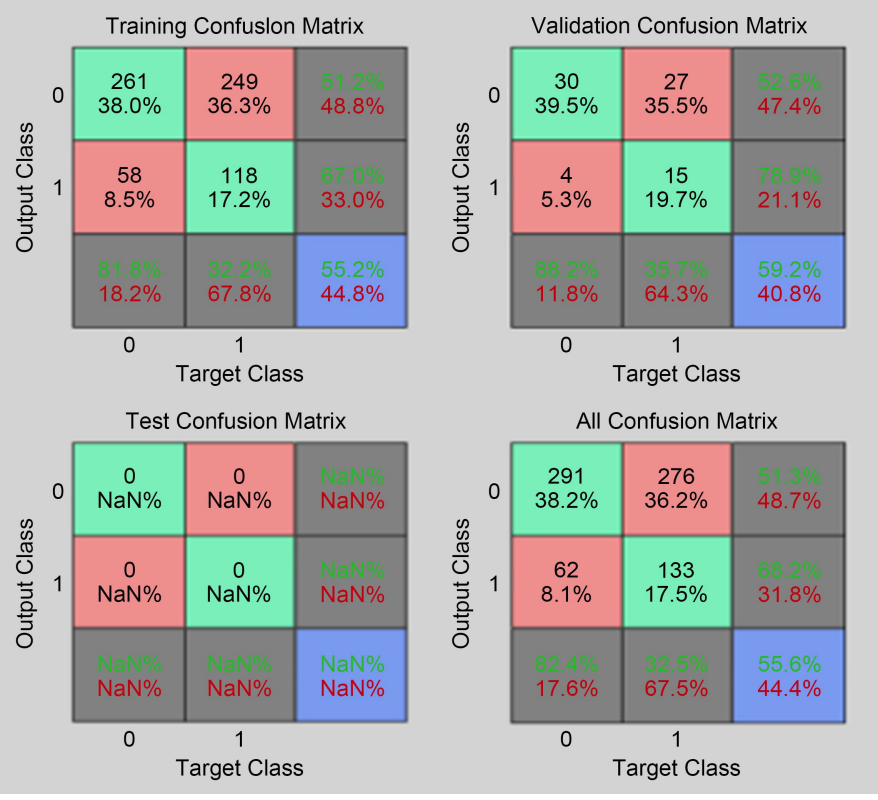


**Figure 10.** Confusion matrix.

Figure 9 presents the Receiver Operating Characteristic (ROC) curves and the corresponding Area Under the Curve (AUC) values. The AUC values, ranging between 0.5 and 1, indicate that the classifier demonstrates strong discriminatory power. Furthermore, the confusion matrix reveals that the classifier is highly reliable, exhibiting very low rates of both false negatives and false positives (Figure 10).

## 5. Discussion

In this study, orthogonal Jacobi polynomials specifically the Legendre polynomials were employed to extract meaningful features from EEG signals collected from healthy subjects and patients with disorders of consciousness (DoC). This approach introduces a novel framework for the detection and diagnosis of DoC by integrating DLT-based spectral features with temporal and statistical descriptors, subsequently used as input to a machine learning classifier. The adoption of a 10-fold cross-validation scheme ensured robustness of the results and mitigated overfitting during model training.

The classification task was conducted in a binary manner, distinguishing healthy individuals from DoC patients. The proposed method achieved an accuracy of 75.44% on the same dataset previously analyzed by *Coralie Joucla*. Although this performance is slightly lower than some existing approaches, our method contributes an innovative feature extraction strategy that enhances traditional time- and frequency-domain EEG analyses.

Table 3: Comparative analysis of previous studies and our work presents a comparative summary of our results with those reported in previous studies, emphasizing the originality and effectiveness of the proposed methodology.

Table 3. Comparative analysis of previous studies and our work.

| Authors/Criteria | Classifier used | Spectral analysis tool | Selection of parameters | Extraction of features | Precision |
|---|---|---|---|---|---|
| Coralie *et al.*, 2020 | Support vector machine | None | Genetic algorithm | Fourier transform | 55% |
| Federico *et al.*, 2018 | Support vector machine | None | None | None | 78% |
| Our work | Artificial neural network | Legendre orthogonal polynomials | Principal component analysis | Discrete transform of legendre | 75.44% |

## 6. Conclusions

In this study, we analyzed EEG recordings from 29 patients with disorders of consciousness and vigilance, and 26 healthy individuals. As expected, based on findings from previous studies, our results confirm several previously reported observations while introducing original contributions.

The originality of this work lies in the characterization of consciousness using orthogonal Legendre polynomials for spectral decomposition and feature extraction. Consciousness comprises two fundamental components: awareness and vigilance. Awareness relates to the perception of the external environment, while vigilance corresponds to wakefulness. Even during wakefulness, the way an individual perceives and responds to a specific stimulus can vary. Moreover, not all conscious experiences occur exclusively during wakefulness, as multiple studies have attempted to uncover the underlying mechanisms of consciousness. Disorders of consciousness in which consciousness is impaired, pose major diagnostic challenges. Diagnosis is often based on bedside assessments, leaving considerable room for misdiagnosis. For instance, a patient with impaired awareness and vigilance may be classified as comatose, yet distinctions become complex when only one of these components is affected, or the level of impairment is subtle.

Patients in a vegetative or unresponsive wakefulness state retain vigilance but lack awareness of self or environment, whereas those in a minimally conscious state maintain both wakefulness and partial, fluctuating awareness. Some patients may transition between states, complicating diagnosis.

The proposed model, based on Discrete Legendre Transform and neural network classification, shows promising results for assisting in differentiating between these states. However, further validation is required using data from multiple clinical centers specializing in disorders of consciousness. Its intended use is to complement, not replace, clinical expertise providing clinicians with an intelligent support tool to enhance diagnostic accuracy and decision-making in the evaluation of consciousness disorders.

## Conflicts of Interest

The authors declare that they have no conflict of interest.

They further state that there are no competing financial interests or personal relationships that could have influenced the work reported in this paper.

## References

[1] Giacino, J.T., Fins, J.J., Laureys, S. and Schiff, N.D. (2014) Disorders of Consciousness after Acquired Brain Injury: The State of the Science. *Nature Reviews Neurology*, **10**, 99-114. https://doi.org/10.1038/nrneurol.2013.279

[2] Schiff, N.D. and Plum, F. (2000) The Role of Arousal and "Gating" Systems in the Neurology of Impaired Consciousness. *Journal of Clinical Neurophysiology*, **17**, 438-452. https://doi.org/10.1097/00004691-200009000-00002

[3] Piarulli, A., Bergamasco, M., Thibaut, A., *et al.* (2016) EEG Ultradian Rhythmicity Differences in Disorders of Consciousness during Wakefulness. *Journal of Neurology*, **263**, 1746-1760. https://doi.org/10.1007/s00415-016-8196-y

[4] Laureys, S., Celesia, G.G., Cohadon, F., Lavrijsen, J., León-Carrión, J., Sannita, W.G., *et al.* (2010) Unresponsive Wakefulness Syndrome: A New Name for the Vegetative State or Apallic Syndrome. *BMC Medicine*, **8**, Article No. 68. https://doi.org/10.1186/1741-7015-8-68

[5] Schnakers, C., Vanhaudenhuyse, A., Giacino, J., Ventura, M., Boly, M., Majerus, S., *et al.* (2009) Diagnostic Accuracy of the Vegetative and Minimally Conscious State: Clinical Consensus versus Standardized Neurobehavioral Assessment. *BMC Neurology*, **9**, Article No. 35. https://doi.org/10.1186/1471-2377-9-35

[6] Comanducci, A., Boly, M., Claassen, J., De Lucia, M., Gibson, R.M., Juan, E., *et al.* (2020) Clinical and Advanced Neurophysiology in the Prognostic and Diagnostic Evaluation of Disorders of Consciousness: Review of an IFCN-Endorsed Expert Group. *Clinical Neurophysiology*, **131**, 2736-2765. https://doi.org/10.1016/j.clinph.2020.07.015

[7] Bai, Y., Lin, Y. and Ziemann, U. (2020) Managing Disorders of Consciousness: The Role of Electroencephalography. *Journal of Neurology*, **268**, 4033-4065. https://doi.org/10.1007/s00415-020-10095-z

[8] Plum, P.J. and Plum, F. (1996) The Diagnosis of Stupor and Coma, Contemporary Neurology Series. Oxford University Press.

[9] Cobb, W.A., Guiloff, R.J. and Cast, J. (1979) Breach Rhythm: The EEG Related to Skull Defects. *Electroencephalography and Clinical Neurophysiology*, **47**, 251-271. https://doi.org/10.1016/0013-4694(79)90278-5

[10] Lau, S., Flemming, L. and Haueisen, J. (2014) Magnetoencephalography Signals Are Influenced by Skull Defects. *Clinical Neurophysiology*, **125**, 1653-1662. https://doi.org/10.1016/j.clinph.2013.12.099

[11] Hirsch, L.J., Fong, M.W.K., *et al.* (2013) American Clinical Neurophysiology Society's Standardized Critical Care EEG Terminology. *Journal of Clinical Neurophysiology*, **30**, 1-27.

[12] Posner, J.B., Saper, C.B., Schiff, N. and Plum, F. (2008) Plum and Posner's Diagnosis of Stupor and Coma. Oxford University Press. https://doi.org/10.1093/med/9780195321319.001.0001

[13] Howard, R.S. (2012) Coma and Brainstem Death. *Medicine*, **40**, 500-506. https://doi.org/10.1016/j.mpmed.2012.06.004

[14] Laureys, S. (2005) Death, Unconsciousness and the Brain. *Nature Reviews Neuroscience*, **6**, 899-909. https://doi.org/10.1038/nrn1789

[15] Westphal, G.A., Garcia, V.D., *et al.* (2016) Guidelines for the Assessment and Acceptance of Potential Brain-Dead Organ Donors. *Revista Brasileira de terapia intensiva*, **28**, 220-255.

[16] Jennett, B. and Plum, F. (1976) Persistent Vegetative State after Brain Damage: A Syndrome in Search of a Name. *The Lancet*, **296**, 734-737.

[17] Giacino, J.T. (2005) The Vegetative and Minimally Conscious States: Consensus-Based Criteria for Establishing Diagnosis and Prognosis. *NeuroRehabilitation*, **19**, 293-298. https://doi.org/10.3233/nre-2004-19405

[18] Lulé, D., Zickler, C., Häcker, S., Bruno, M.A., Demertzi, A., Pellas, F., *et al.* (2009) Life Can Be Worth Living in Locked-In Syndrome. *Progress in Brain Research*, **177**, 339-351. https://doi.org/10.1016/s0079-6123(09)17723-3

[19] Bruno, M.-A., Pellas, F., Bernheim, J.-L., *et al.* (2008) Quelle vie après le Locked In Syndrome ? *Revue Médicale de Liège*, **63**, 445-451.

[20] Leon-Carrion, J., Martin-Rodriguez, J.F., Damas-Lopez, J., Barroso y Martin, J.M. and Dominguez-Morales, M.R. (2008) Brain Function in the Minimally Conscious State: A Quantitative Neurophysiological Study. *Clinical Neurophysiology*, **119**, 1506-1514. https://doi.org/10.1016/j.clinph.2008.03.030

[21] Lehembre, R., Gosseries, O., *et al.* (2012) Electrophysiological Investigations of Brain

Function in Coma, Vegetative and Minimally Conscious Patients. *Archives Italiennes de biologie*, **150**, 2-3.

[22] Marsden, C. (1981) The Diagnosis of Stupor and Coma, 3rd Ed. *Journal of Neurology, Neurosurgery & Psychiatry*, **44**, 270-271. https://doi.org/10.1136/jnnp.44.3.270-a

[23] Bagnato, S., Boccagni, C., Sant'Angelo, A., Prestandrea, C., Mazzilli, R. and Galardi, G. (2015) EEG Predictors of Outcome in Patients with Disorders of Consciousness Admitted for Intensive Rehabilitation. *Clinical Neurophysiology*, **126**, 959-966. https://doi.org/10.1016/j.clinph.2014.08.005

[24] Monti, M.M., Laureys, S. and Owen, A.M. (2010) The Vegetative State. *BMJ*, **341**, c3765. https://doi.org/10.1136/bmj.c3765

[25] Klimesch, W. (1999) EEG $\alpha$ and Theta Oscillations Reflect Cognitive and Memory Performance: A Review and Analysis. *Brain Research Reviews*, **29**, 169-195. https://doi.org/10.1016/s0165-0173(98)00056-3

[26] Busch, N.A. and VanRullen, R. (2010) Spontaneous EEG Oscillations Reveal Periodic Sampling of Visual Attention. *Proceedings of the National Academy of Sciences of the United States of America*, **107**, 16048-16053.

[27] Lechinger, J., Bothe, K., Pichler, G., Michitsch, G., Donis, J., Klimesch, W., *et al.* (2013) CRS-R Score in Disorders of Consciousness Is Strongly Related to Spectral EEG at Rest. *Journal of Neurology*, **260**, 2348-2356. https://doi.org/10.1007/s00415-013-6982-3

[28] Bai, Y., He, J.H., Xia, X.Y., *et al.* (2015) Spontaneous Transient Brain States in EEG Source Space in Disorders of Consciousness. *Proceedings of the National Academy of Sciences*, **240**, Article ID: 118407.

[29] Sitt, J.D., King, J., El Karoui, I., Rohaut, B., Faugeras, F., Gramfort, A., *et al.* (2014) Large Scale Screening of Neural Signatures of Consciousness in Patients in a Vegetative or Minimally Conscious State. *Brain*, **137**, 2258-2270. https://doi.org/10.1093/brain/awu141

[30] Joucla, C. (2020) Électroencéphalographie et machines à vecteurs de support dans le diagnostic différentiel des pathologies neuropsychiatriques: État des lieux, enjeux et applications. Master's Thesis, Université Bourgogne.

[31] Naro, A., Bramanti, A., Leo, A., Cacciola, A., Manuli, A., Bramanti, P., *et al.* (2018) Shedding New Light on Disorders of Consciousness Diagnosis: The Dynamic Functional Connectivity. *Cortex*, **103**, 316-328. https://doi.org/10.1016/j.cortex.2018.03.029